CHEMISTRY
A EUROPEAN JOURNAL

DOI: 10.1002/chem.200700505

A Mononuclear Cyclopentadiene–Iron Complex Grafted in the Supercages of HY Zeolite: Synthesis, Structure, and Reactivity

Jinlin Long, Xuxu Wang, Guoying Zhang, Jingguo Dong, Tingjiang Yan, Zhaohui Li, and Xianzhi Fu*[a]

Abstract: The reaction of ferrocene with the acidic hydroxy groups in the supercages of zeolite HY dehydrated at 673 K and the reactivity of the resultant surface species towards CO and O_2 were investigated by temperature-programmed decomposition (TPD) and reduction (TPR) and IR, X-ray absorption fine structure analysis (XAFS), and X-ray photoelectron (XP) spectroscopy. In situ FTIR, TPD, TPR, and chemical analysis reveal that the Cp_2Fe molecule adsorbed on the zeolite surface loses one cyclopentadienyl group under vacuum at 423 K, which leads to the formation of a well-defined mononuclear surface Fe-C_5H_6 complex grafted to two acidic sites and one (≡Si-O-Si≡) unit, as confirmed by the lack of Fe–Fe contributions in the EXAFS spectra. Each iron atom is coordinated, on average, to three oxygen atoms of the zeolite surface with a Fe–O distance of 2.00 Å and to five carbon atoms with a Fe–C distance of 2.09 Å. IR spectra indicate that the cyclopentadiene–iron species grafted on the surface of the zeolite is quite stable in vacuo or under an inert or hydrogen atmosphere below 423 K, and is also relatively stable under oxygen at room temperature. However, the cyclopentadiene ligand readily reacts with CO to form a compound containing carbonyl at 323 K, and even at room temperature. The single carbonyl band in the IR spectra provides evidence for the nearly uniform formation of a cyclopentadiene–iron species on the surface of the zeolite.

Keywords: immobilization · iron · sandwich complexes · surface chemistry · zeolites

Introduction

The use of organotransition metal complexes as catalysts and precursors of active catalysts is an exciting field of research that, in the last decade or so, has led to revolutionary changes in organic synthesis.[1] Many moisture-sensitive organometallic compounds can react with solid surfaces to form surface organometallic fragments that are close analogues of molecular complexes, with the bonding between and metal and the oxygen atoms of the support being strong enough to maintain anchoring during catalysis.[2–4] In some cases, these grafted organometallic catalysts show substantially enhanced reactivity, stability, and selectivity compared to the parent compounds.[5,6] Some surface organometallic complexes with unique local environments probably provide molecular insights into the "elementary steps" of heterogeneous catalysis.

The supports play a critical role in constructing unique surface organometallic complexes. Zeolites, especially large-pore zeolite Y (faujasite), can offer great advantages over other oxide supports including silica and alumina because the former has a high degree of uniformity, adjustable acidic properties, and a strong electrostatic field inside its cages,[7] while the latter lack these features. Furthermore, these intrinsic properties may be helpful to the stable existence of the surface organometallic complex.

Iron is one of the most abundant metals on earth and consequently one of the most inexpensive and environmentally friendly ones.[8] Organometallic iron complexes, such as iron carbonyls, ferrocene and its derivatives, Fe–porphyrins etc., have received particular attention due to their utility as homogeneous catalysts for C–H oxidation[9] and olefin epoxidation,[10] especially for cycloaddition reactions of unsaturated molecules in organic syntheses,[11] which is often considered an ideal chemical reaction in terms of atom econo-

[a] J. Long, Prof. X. Wang, G. Zhang, J. Dong, T. Yan, Prof. Z. Li, Prof. X. Fu
Research Institute of Photocatalysis
State Key Laboratory Breeding Base of Photocatalysis
Fuzhou University, Fuzhou, 350002 (China)
Fax: (+86) 591-8373-8608
E-mail: xzfu@fzu.edu.cn

Supporting Information for this article is available on the WWW under http://www.chemeurj.org/ or from the author.

my.[12] Substantial effort has therefore been devoted to understanding the structure and reactivity of iron carbonyls bonded to zeolites and metal oxides over last decade.[13] However, these supported catalysts have, for the most part, suffered from lack of activity because of the relatively unreactive nature of the carbonyl ligands remaining bonded to the iron center.

Dienes have been used as the active ligand in transition-metal complexes due to their special reactivity.[14] Significantly, the diene was found to facilitate the cycloaddition reaction relative to an alkene. In the case of the [2+2+1] cycloaddition reaction of diene-enes, for example, the presence of the diene enabled the reaction to occur,[15] and the formation of a diallene–iron intermediate plays a crucial role in the iron-catalyzed [4+1] cycloaddition of diallenes with carbon monoxide.[16] These findings inspired us to look for synthetic routes to a diene–iron complex intermediate because of its likely role as a catalytic intermediate.

Ferrocene, which is used to construct such a catalytic intermediate, is a perfect precursor due to its two cyclopentadienyl groups. The intrazeolite chemistry, spectroscopy, and dynamics of metallocenes such as Cp_2Fe, Cp_2Cr, and Cp_2Co, and intrazeolite half-sandwich carbonyl compounds of iridium and rhodium, have been studied in detail,[17] and $[CpFe(CO)_2(thf)]^+$ anchored to mesoporous silica has been used as an adsorbent for the removal of dibenzothiophenes.[18] It is worth noting that similar intrazeolite transformations have been proposed to yield half-sandwich organometallic fragments by the reactions of $[(cot)Fe(CO)_3]$ (cot = cyclooctatriene) and $[\{CpFe(CO)_2\}_2]$ with acid zeolites.[19] These investigations suggested the need for a study to better understand the chemical nature of these so-called half-sandwich organometallic complexes inside a zeolite.

Herein we report the synthesis, structure, and reactivity of a well-defined mononuclear diene–iron complex that is bonded to the acidic sites of zeolite HY by a grafting reaction between ferrocene and the surface of the zeolite. This iron species is stable in vacuo or under an inert or hydrogen atmosphere up to a temperature of 473 K. The IR spectra show that the complex is highly reactive towards CO and O_2 at 298–423 K. Its structure and bonding are well characterized by IR spectroscopy and XAFS in combination with X-ray photoelectron spectroscopy (XPS).

Results

In situ IR study of the reactivity of ferrocene towards HY zeolite: NH_4Y zeolite was calcined at 793 K under flowing oxygen for 20 h and then heated under dynamic vacuum at 673 K for 3 h. The IR spectrum of the resulting solid shows three classical hydroxy vibration adsorption bands at 3740 (isolated silanol groups), 3638 (acid hydroxy groups in the supercages), and 3546 cm^{-1} (acid hydroxy groups in the sodalite cages or in the hexagonal prisms) (Figure 1b).[20] The absence of N–H bands shows that all ammonium ions have been converted into protons.

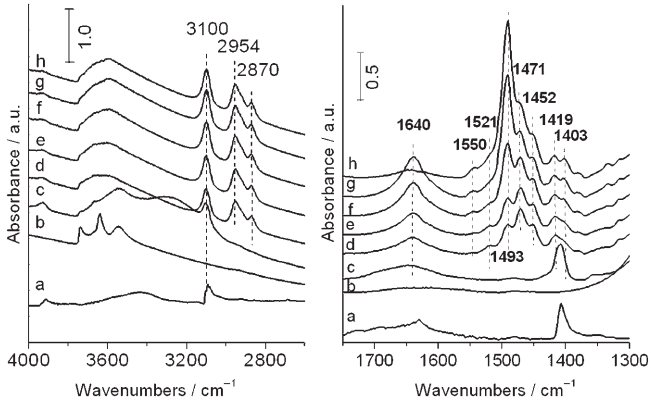

Figure 1. In situ FTIR spectra of HY zeolite before and after grafting of Cp_2Fe: a) ferrocene; b) HY zeolite dehydrated at 673 K in vacuo; c) after adsorption of ferrocene at room temperature; d) after heating at 423 K for 5 h, e) for 15 h, f) for 30 h, and g) for 45 h; h) elimination of the physisorbed species at 423 K in vacuo.

Introduction of Cp_2Fe (Cp: η^5-C_5H_5) by sublimation resulted in a decrease in the absorption intensities of the silanol bands and the Brönsted acid hydroxy bands at 3638 cm^{-1} (Figure 1c) and the appearance of a new broad adsorption at around 3300 cm^{-1}, thus indicating hydrogen bonding between the zeolite OH groups and the adsorbed ferrocene. The appearance of new C–H stretching (at 3100 cm^{-1}) and C=C adsorptions (at 1408 cm^{-1}), which are in good agreement with those of Cp_2Fe (Figure 1a),[21] is also clearly observed. The color of the sample changes from white to yellow, which further indicates that the Cp_2Fe molecules are only adsorbed onto the external surface of the HY zeolite and the acidic sites in the supercages (hereafter denoted as Cp_2Fe/HY).

When the above system is heated at 423 K the sample gradually becomes bright green and the IR spectrum changes drastically. Two new IR bands (Figure 1d–g) in the region 2953 and 2873 cm^{-1}, which are assigned to the stretching vibrations of a methylene group, and seven new IR bands at 1640, 1521, 1491, 1471, 1452, 1419, and 1403 cm^{-1} (Figure 1d–g) in the region 1400–1700 cm^{-1} due to the vibration modes of olefinic C=C and methylene, are clearly observed. These bands are very different from those of Cp_2Fe,[22] Cp_2Fe absorbed on the surface of HY zeolite (Figure 1c), and ferricinium ion (Cp_2Fe^+).[22] This shows unambiguously that Cp_2Fe reacts with the zeolite at this temperature. After heating at 423 K for five hours, the hydrogen-bonding band at around 3300 cm^{-1} had disappeared completely and the intensity of the band at 3100 cm^{-1} had increased significantly; the band at 1408 cm^{-1} had also disappeared (Figure 1d). The intensities of the bands at 2953, 2873, 1521, 1492, 1471, and 1452 cm^{-1} increased gradually with increasing reaction time. After heating at 423 K for 45 h and evacuation at the same temperature under dynamic vacuum to remove physisorbed species, the sample showed no further change in the main absorption bands except for that at 1640 cm^{-1} (Figure 1h), which is attributed to the C=

C stretching mode of an alkene.[23] This suggests a complete reaction between the surface acidic hydroxy groups in the supercages and Cp_2Fe. The band at 1640 cm^{-1} is probably therefore due to gaseous products containing a C=C bond and physisorbed Cp_2Fe. The almost complete disappearance of this band is indicative of the complete removal of these species. The new band at around 1550 cm^{-1}, which is weak and remains unaltered after evacuation of the sample, is a "coke band" due to the C=C vibration of polyalkenes and/or aromatic structures.[24] It can thus be concluded that Cp_2Fe is destroyed by the grafting reaction. The adsorption and reactivity of Cp_2Fe on the surface of HY zeolite were also confirmed by the interaction of Cp_2Fe with DY (deuterated Y zeolite), as shown in Figure S1 in the Supporting Information.

A further experiment was performed with a larger amount of zeolite to determine the nature of the products evolved and the chemical composition of the remaining solid. GC-MS studies showed that numerous gaseous products such as cyclopentane, methylcyclobutane, and cyclopentene are formed during the grafting reaction (see Figure S2 in the Supporting Information). These hydrocarbons could be formed by reaction of the cyclopentadiene derived from addition of one cyclopentadienyl group of ferrocene to acidic hydroxy groups catalyzed by H^+ sites, as discussed in further detail below. Chemical analysis of the solid remaining after complete elimination of the physisorbed species gave a C/Fe ratio of 5.35 (C: 1.26 wt%; Fe: 1.10 wt%), which is basically in agreement with the loss of one cyclopentadienyl ligand during the reaction. The surplus carbon shows up as a few small carbon deposits on the zeolite surface, in accordance with the IR results.

TPD-MS and TPR-MS studies on the thermal decomposition of ferrocene adsorbed on HY zeolite and the grafted sample: The results of temperature-programmed decomposition (TPD) studies carried out under flowing He are shown in Figure 2. The most important fragments detected between 423 and 750 K for the Cp_2Fe/HY sample (Figure 2 A) are C_5H_6 (*m*/*z* 66) and $C_5H_5^{\cdot}$ (*m*/*z* 65), with no evidence for Cp_2Fe^+ ion, Cp_2Fe (*m*/*z* 186), or $CpFe^{\cdot}$ (*m*/*z* 121), which shows that decomposition of Cp_2Fe on the zeolite occurs in this temperature range. The TPD patterns of C_5H_6 and $C_5H_5^{\cdot}$ present double release peaks. Interestingly, the area ratio of the peak centered at 503 K and that centered at 553 K is close to 1:1 for each discharge product, with a decomposition onset temperature of 423 K. This clearly indicates that Cp_2Fe remains intact below 423 K and that the reaction of Cp_2Fe with HY zeolite occurs in two steps beyond 423 K, This is in good agreement with the IR results. In contrast to $FeCp_2$/HY, the grafted sample, which was prepared by heating Cp_2Fe/HY at 423 K for 50 hours, only shows a single release peak for C_5H_6 and $C_5H_5^{\cdot}$ at 553 K (Figure 2B) which is identical to the second peak in the Cp_2Fe/HY sample. This supports the deduction that a C_5H_6-Fe or C_5H_5-Fe species is formed on the surface of the zeolite in the grafted sample by loss of a cyclopentadienyl group from

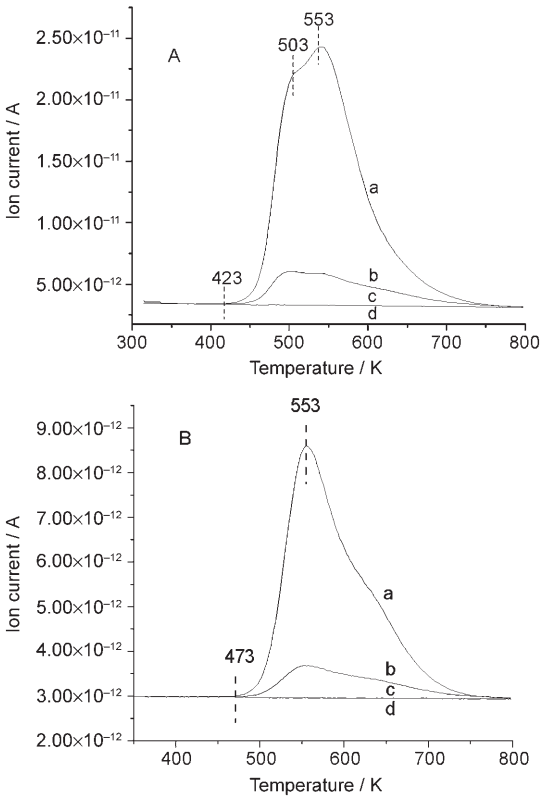

Figure 2. TPD-MS plots of ferrocene adsorbed on HY zeolite (A) and the grafted sample (B). a) *m*/*z* 66; b) *m*/*z* 65; c) *m*/*z* 121; d) *m*/*z* 186.

Cp_2Fe, thus confirming the IR results above. The decomposition onset temperature of the grafting sample is at about 473 K, which suggests that the surface-grafted species is stable below this temperature. This is also basically consistent with the observations made by IR spectroscopy (see Figure S3 in the Supporting Information).

The temperature-programmed reduction (TPR) analysis of the grafted sample further confirms the above conclusions. As shown in Figure 3, C_5H_6 and $C_5H_5^{\cdot}$ fragments, which are fully consistent with the TPD result, and C_5H_8 (*m*/*z* 68) and C_5H_{10} (*m*/*z* 70) fragments, which are derived

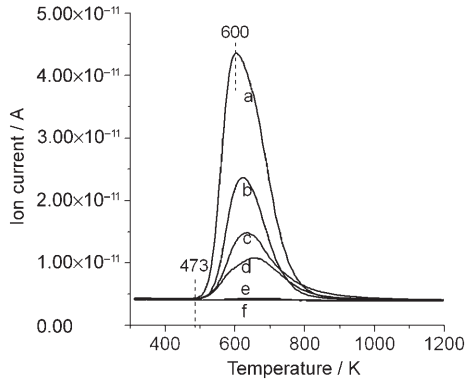

Figure 3. TPR-MS plot of the grafted sample: a) *m*/*z* 66; b) *m*/*z* 68; c) *m*/*z* 70; d) *m*/*z* 65; e) *m*/*z* 121; f) *m*/*z* 186.

from the hydrogenation of cyclopentadiene under H_2/Ar flow, are detected between 473 and 900 K. The reduction onset temperature is also fully consistent with the decomposition onset temperature, thus indicating that the surface-grafted species is also stable in the presence of hydrogen below 473 K.

XAFS analytical results regarding the local structure of the surface iron complex: The local structure of the surface iron complex was characterized by X-ray absorption spectroscopy. Fe K-edge XAFS data were obtained for Cp_2Fe, Cp_2Fe/HY, and the grafted sample. The XAFS data of Fe/Y are used as a reference. The normalized XANES spectra collected at the Fe K-edge for these three samples are shown in Figure 4, with the inset showing an expanded view of the

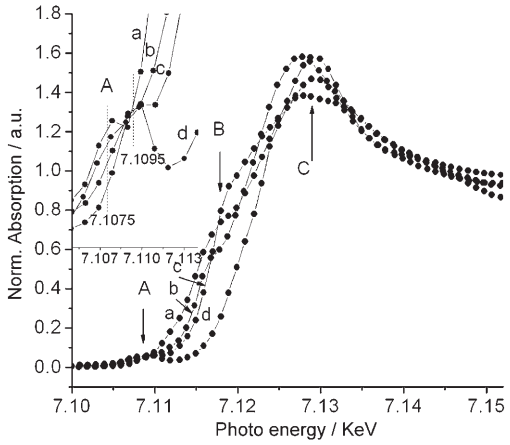

Figure 4. Normalized Fe K-edge XANES spectra of the grafted sample and the studied materials: a) Cp_2Fe; b) Cp_2Fe/HY; c) the grafted sample; d) Fe/Y zeolite. See text for details about A–C and the insert.

1s→3d pre-edge region. All three samples show a weak pre-edge feature (A), a distinguishable shoulder (B), and a peak (C).

A 1s→3d transition is electric dipole forbidden by parity considerations for Cp_2Fe and Cp_2Fe/HY due to their centrosymmetric environment.[25] However, a very weak pre-edge feature at about 7107.5 eV is still experimentally observed for these two samples. The most likely intensity mechanism is the allowed electric quadrupole coupling transition to the lowest unoccupied level 5e1g,[26] which corresponds principally, according to Rösch and Johnson,[27] to an Fe ($3d_{xz}$,$3d_{yz}$)-like orbital. In contrast to these two samples, a more intense pre-edge feature, which shifts toward high energy, is clearly observed at 7109.5 eV for the grafted sample. This shift, along with the increase in intensity, is attributed to loss of the centrosymmetric environment of the iron upon grafting of ferrocene to HY zeolite.

The position of the rising K-edge, where a 1s electron is promoted to the continuum, depends on the effective charge of the metal center and is thus directly related to the oxidation state of the absorbing atoms—it moves to higher energy as the oxidation state of the absorbing atoms increases.[28] As shown in Figure 4, the absorption edge energy of Fe/Y zeolite is far higher than that of the other three samples because iron exists in the form Fe^{3+}.[29] Although the absorption edge shifts slightly toward higher energy in Cp_2Fe/HY and the grafted sample, no overall significant shift of the absorption edge can be detected, thus showing that there is no change in the oxidation state of iron, which remains as Fe^{2+}. This was also confirmed by the XPS analytical results below. Additionally, the pre-edge position of iron shifts towards higher energy by about 2.0 eV after the grafting reaction. According to the absorption edge position and the XPS results, we can exclude the contribution arising from Fe^{3+} and conclude that this shift may be related to oxygen ligation. The lack of change in the oxidation state of iron further proves that the reaction of ferrocene with HY zeolite is only a grafting reaction rather than a redox reaction.

The shoulder B (see Figure 4) located on the adsorption edge is assigned to a "shape" resonance in the continuum of states whose resolution is quite sensitive to small variations of the metal–carbon bond length.[26] It is noteworthy that the intensity of this shoulder is higher for the grafted sample than for ferrocene and its resolution improves accordingly, which indicates that the Fe–C bond length increases after the reaction. This is in agreement with the EXAFS analytical results below.

The Fe K-edge K^3-weighted EXAFS spectra of the grafted sample and Cp_2Fe/HY, together with that of ferrocene as reference, are shown in Figure 5 and Table 1. All Fourier transform (FT) values are uncorrected for phase shifts. The FT of the ferrocene precursor serves as a standard to estimate relative changes between the samples. It can be seen from Figure 5 that the first peak in the FT is shifted to a higher radial distance for the grafted sample relative to the ferrocene spectrum. This shift in the first-shell peak distance indicates a change in the first-shell carbon distance (Fe–C) from 2.06 Å in ferrocene to 2.09 Å in the grafted sample. The first peak at about 1.7 Å (uncorrected), which is presumably due to the Fe–C shell from FeC_5H_x, was back-filtered through a range of 1.1–2.1 Å, although this gave only a poor fit. However, if an Fe–O shell is also considered to be present an acceptable fit can be achieved with an Fe–C distance of 2.09 Å and an Fe–O distance of 2.0 Å. Analysis of the Fe-K edge EXAFS data of the grafted sample gives a first coordination sphere of three O atoms at 2.0 Å and five C atoms at 2.09 Å. Despite the similarity of O and C phase-shifts, attempts to fit an O shell at 2.09 Å together with a C shell at 2.00 Å result in significantly increased refinement (R) factors and unacceptable Debye–Waller factors for these two shells. Although the quality of the data certainly limits the precision of this distant shell, the Fe–O distance is similar to those observed in iron(III) acetylacetonate (1.99 Å)[30] and $C_4H_6Fe(CO)_3{\cdot}SO_2{\cdot}BF_2$ (2.00 Å).[31] The Fe–C distance lies between those of ferrocene (2.06 Å) and Fe–alkene (2.14–2.16 Å),[32] and is close to that of tricarbonyl tetraphenylacetylcyclobutadieneiron (2.08 Å).[33] The

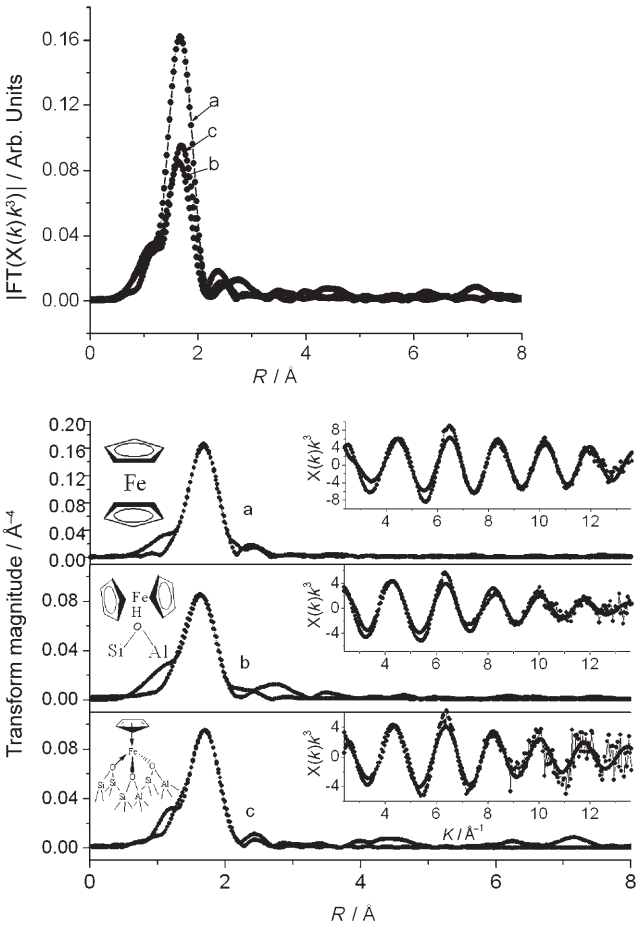

Figure 5. The Fe K-edge K^3-weighted EXAFS spectra of: a) Cp_2Fe, b) Cp_2Fe/HY, and c) the grafted sample. The insert shows the experimental and fitted K^3-weighted scattering functions.

EXAFS results thus strongly support the presence of a mononuclear $(\equiv Si\text{-}O\text{-}Al(OSi)\equiv)_3Fe\text{-}C_5H_x$ surface species.

Oxidation state of the surface iron complex: A comparison of the XPS spectra of Cp_2Fe/HY and the grafted HY sample (Figure 6) shows that the peak positions and widths of $Fe\,2p_{3/2}$ are essentially the same, which suggests that the oxidation state of ferrocene before and after the reaction does not change. The binding energies of $Fe\,2p_{3/2}$ and $Fe\,2p_{1/2}$ are 709.6 and 723.0 eV, respectively, for the Cp_2Fe/HY sample, while the respective values for the grafted sample shift

Table 1. EXAFS fit parameters used to characterize the grafted sample.[a]

Sample	Shell	CN	R [Å]	δ^2 [Å]	ΔE_0 [eV]
Cp_2Fe	Fe–C	10.0	2.06	0.00036	10.88
Cp_2Fe/HY	Fe–C	10.4	2.07	0.0086	4.97
	Fe–C	5.2	2.09	0.0040	1.69
$CpHFe/(OZ\equiv)_3$	Fe–O	3.0	2.00	0.0090	17.77

[a] Notation: CN: coordination number; R: absorber-backscatter distance; δ^2: Debye–Waller factor relative to that of the reference compound; ΔE_0: inner potential correction. Approximate experimental uncertainties: CN: ±10%; R: ±10%.

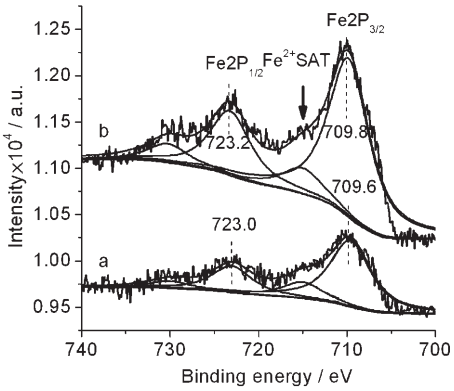

Figure 6. XPS spectra of Cp2Fe/HY (a) and the grafted HY sample (b). The solid lines correspond to the fitted lines.

toward high energy by 0.2 eV, which is clearly due to the strong interaction of iron with the zeolite support. This is strong evidence in support of the proposal that one cyclopentadienyl group of ferrocene is replaced by the framework oxygen atoms in the acid sites upon heating, which would lead to the observed increase in the $Fe\,2p_{3/2}$ binding energy. Although the $Fe\,2p_{3/2}$ binding energy in these two samples is much higher than that of ferrocene (707.9 eV),[34] a broad shake-up satellite at about 715 eV, which is characteristic of a Fe^{2+} species,[35] is clearly observed for these two samples. The combined use of the main $2p_{3/2}$ line and its satellite, plus the spin-orbit splitting energy of 12.6 eV, provide a reliable identification of Fe^{3+} and Fe^{2+} species, thus indicating that iron remains in the divalent state after the grafting reaction.

Reactivity of the surface iron complex: Monitoring the change of the surface iron species in the presence of CO at ambient temperature by IR spectroscopy (Figure 7) showed that the characteristic C–H and C=C vibrations in the region 1300–1800 cm^{-1} are strongly affected, while the vibrations in the region 2700–3300 cm^{-1} remain almost unchanged. The bands at 1493, 1471, and 1521 cm^{-1} decrease in intensity with increasing concentration of CO and a new IR band, corresponding to the ν(C=O) stretching mode, appears at 1707 cm^{-1}, the intensity of which increases with increasing concentration of CO. The changes in the IR spectra become clearer with increasing reaction temperature (Figure 8). Thus, the ν(C=O) stretching mode at 1707 cm^{-1} and the ν(C=C) stretching mode at 1640 cm^{-1} become stronger and the bands at 1452, 1493, 1471, and 1521 cm^{-1} almost disappear, which indicates that the surface iron complex reacts with CO to form a cyclopentadiene ligand containing a C=O bond. This observation provides valuable information for further identifying the

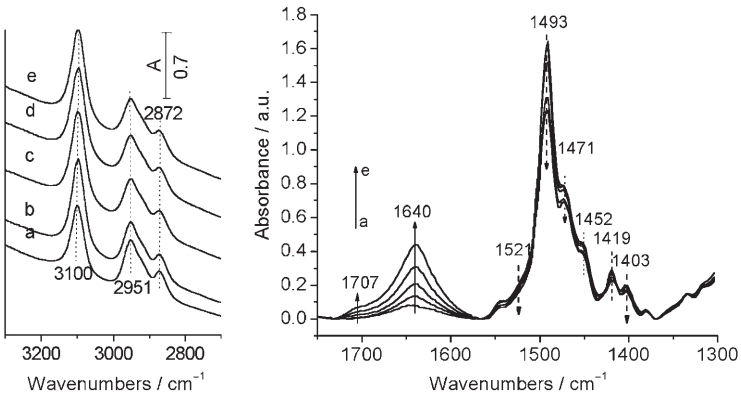

Figure 7. IR spectra of the grafted sample upon treatment with CO at room temperature: a) $P_{(CO)}=0$ kPa; b) $P_{(CO)}=0.675$ kPa; c) $P_{(CO)}=1.35$ kPa; d) $P_{(CO)}=2.7$ kPa; e) $P_{(CO)}=4.05$ kPa.

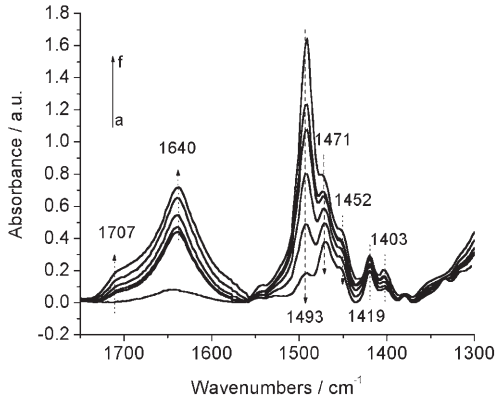

Figure 8. IR spectra of the grafted sample upon treatment with CO at high temperature: a) the grafted sample; b) $P_{(CO)}=4.05$ kPa at room temperature; c) after reaction at 323 K for 3 h; d) after reaction at 353 K for 2 h; e) after reaction at 373 K for 2 h; f) after reaction at 373 K for 10 h.

surface species and its structure, and suggests the likely role of the cyclopentadiene ligand as an intermediate in catalytic addition or insertion reactions. This reaction also provides evidence for the "molecular nature" of iron-catalyzed [4+1] addition or CO insertion reactions.

Discussion

Synthesis and structure of the surface Fe-(η^4-C_5H_6) complex: The size of the supercage in zeolite Y, which contains 12-ring windows of approximately 7.5 Å and a diameter of 12.5 Å, is more than that of ferrocene, which has a kinetic diameter of 4.862×5.170 Å^2.[17b] Ferrocene molecules can therefore enter into the supercages of HY zeolite by internal diffusion and become physisorbed on the acidic sites at room temperature. The IR spectrum (Figure 1c) of this compound indicates that the adsorbed Cp_2Fe remains intact and is not oxidized to ferricenium cation (Cp_2Fe^+) under vacuum. The easy removal of the adsorbed Cp_2Fe under dynamic vacuum at 298 K also supports this conclusion. Adsorption of Cp_2Fe on deuterated Y zeolite (see Figure S1b in the Supporting Information) gives a compound that shows a weak IR band at 2300 cm^{-1}, which corresponds to the C–D stretching vibration and indicates that exchange of the H atoms on the cyclopentadienyl rings of ferrocene for H or D occurs in the supercages. This is in good agreement with earlier reports on the chemistry of Cp_2Fe in Y zeolite.[17b]

Ferrocene does not decompose thermally below 743 K, and even catalytic hydrogenation of the ferrocene molecule over platinum appears to be unsuccessful.[36] This high stability is due to its unique molecular structure and bonding. However, although ferrocene is stable in air, it is easily oxidized to the ferricenium cation Cp_2Fe^+ in solution,[37] and even Cp_2Fe adsorbed on NaY, HY, and MCM-41 can be oxidized to Cp_2Fe^+ by oxygen at room temperature.[38,39] Ozin et al.[17b] have suggested that the ferrocene adsorbed onto Y-type zeolite under vacuum conditions at ambient temperature could transform into Cp_2Fe^+ upon transfer of a proton in the supercages to the cyclopentadienyl ring of ferrocene, followed by interaction with another Brönsted acid site to lead to the formation of H_2O. This is inconsistent with our observations in vacuo at room temperature. The reason for this discrepancy is unknown.

Heating Cp_2Fe/HY at 423 K for 45 h results in striking changes in the IR spectra (Figure 1f). The appearance of several strong IR bands in the region 1400–1700 cm^{-1} is a strong indication of changes in the structure of ferrocene and suggests the formation of a novel surface iron complex. The structure of this surface complex is indicated by the elemental analysis and its spectral and chemical properties. It is not difficult to assign the absorptions in the infrared spectra at 1491, 1471, and 1452 cm^{-1} unambiguously. Thus, the medium band at 1471 cm^{-1} is in good agreement with that of the compound cyclopentadieneiron tricarbonyl despite the difference in the absorption bands in the region 2800–3000 cm^{-1}.[40] In addition, similar absorption bands appear at 1492 and 1462 cm^{-1} in a $Rh(\eta^3\text{-}C_3H_5)_2$ complex grafted on silica.[41] The IR bands at 1491 and 1471 cm^{-1} can therefore be assigned to $\delta(CH_2)$, while the low frequency C–H stretching mode at 1452 cm^{-1} may be attributed to a methylene H_α interaction with the iron atom or the framework oxygen atom of HY. This splitting of the $\delta(CH_2)$ mode into three IR bands probably originates from an iron-cation-induced dipole polarization in cyclopentadiene, which would affect the cyclopentadiene vibration modes observed in the IR spectra. In addition, these CH_2 bands possibly contain a contribution from dimers of cyclopentadiene, which are easily formed in a Diels–Alder reaction, adsorbed chemically on the zeolite surface. This possibility cannot be completely excluded from the IR results alone because this dimer also contains methylene groups. Cyclopentadiene can spontaneously dimerize to dicyclopentadiene in a Diels–Alder reaction even at room temperature, and the rate of this dimerization increases with temperature. The dimerization of cyclopentadiene is a thermodynamically reversible reaction, therefore if the temperature is raised to about the

boiling point of dicyclopentadiene (443 K), the reaction is reversed and the dimer is reconverted into the monomer.[42] The grafting reaction in this study was carried out at 423 K, which is close to the boiling point of dicyclopentadiene, and was followed by treatment under dynamic vacuum at 423 K. It is therefore clear that the amount of dicyclopentadiene remaining on the surface of the Y zeolite should be very low since the majority will have cracked to form cycloalkanes, which are detected by GC-MS, or have reconverted into the monomer. However, according to the EXAFS and element analysis results, the surface organic species coordinated to iron is not a dicyclopentadiene. The reactivity of the surface species towards oxygen strongly supports this conclusion due to the easy oxidation of the ligand under an atmosphere of oxygen. As shown in Figures S4 and S5 in the Supporting Information, the surface species can be easily oxidized by oxygen at 323 K. This behavior is very similar to that of cyclopentadiene, whereas dicyclopentadiene is very stable towards oxygen.[42] The reactivity of the organic species towards CO is also powerful evidence for the above deduction.

The EXAFS fitting results show five C and three O scattering atoms around the iron absorber for the grafted sample. However, this does not accurately reflect the actual number of C atoms coordinated to iron (four or five), and hence it is very difficult to distinguish between cyclopentadienyl and cyclopentadiene only by means of the EXAFS data. Characterization of the surface complex by ^{1}H and ^{13}C solid-state NMR spectroscopy does not give any useful information due to the strong paramagnetic interference from iron. However, the reactivity of the surface species with CO further indicates that the surface organic group is a cyclopentadiene molecule as this type of reactivity was not observed for the CpFe complex anchored to the surface of silica reported by Spoto et al.[43] It is therefore clear that the surface organic group is a cyclopentadiene rather than a cyclopentadienyl ligand.

The analogous surface complexes $(\equiv SiO)_3Ti(\eta^5\text{-}C_5H_5)$ and η^5-CpFe$(OZ\equiv)_{2-3}$ (Z = Si, or Al) have been reported in the literature by grafting Cp_2TiCl_2 to MCM-41 and anchoring $[CpFe(CO)_2]_2$ to HY, respectively at 373–473 K.[19b,44] The calculated structures of this $(\equiv SiO)_3Ti(\eta^5\text{-}C_5H_5)$ intermediate were not, however, in agreement with the experimental EXAFS structure, and force field calculations suggested that the cyclopentadienyl ring is not exactly η^5-bonded to Ti due to steric interactions of the ring with nearby silanols.[45] As for HY zeolite as support, the stronger interaction of the acidic hydroxy groups in the cavities as electron acceptor with the cyclopentadienyl ring may result in the transfer of a proton to the ring. The presence of methylene bands in the IR spectra strongly supports the above deduction. The species on the surface of HY zeolite can therefore be inferred to be cyclopentadiene–iron rather than cyclopentadienyliron.

On the basis of the evidence discussed above, the reaction of Cp_2Fe on HY zeolite can be understood as occurring as follows (Scheme 1). The precursor ferrocene is first adsorbed at two acidic hydroxy sites and the bridging oxygen of the ≡Si-O-Si≡ unit at room temperature. This is followed by a grafting reaction upon heating at 423 K, which leads to the loss of one cyclopentadiene moiety by an addition reaction of ferrocene with acidic protons to form a cyclopentadiene ligand η^4-coordinated to iron. The CpHFe moiety is anchored to two acid sites and one ≡Si-O-Si≡ unit. However, we were only able to detect cyclopentene, cyclopentane, and carbon deposits during the grafted reaction rather than cyclopentadiene itself. This can be explained by disproportionation, oligomerization, and cracking of the newly formed cyclopentadiene and subsequent isomerization catalyzed by the acid sites of the zeolite. It is well known that cyclopentadiene is a very unstable unsaturated cyclohydrocarbon that can disproportionate into cyclopentene and then further into cyclopentane, cyclopentadiene, and polycyclic hydrocarbons in an acid-catalyzed process.[46a] It can also polymerize in a Diels–Alder reaction into a dimer or polymer,[46] which are then cracked into cyclopentene and cyclopentane at the acid sites. To further elucidate how these cycloalkanes are formed we performed an experiment involving desorption of cyclopentadiene adsorbed on HY zeolite in an He flow. The results showed that a large amount of cyclopentane and cyclopentene are formed at a temperature of about 450 K (see Figure S6 in the Supporting Information) along with small deposits of carbon[47]) and a small amount of low molecular weight hydrocarbons such as methane, ethane, and propane, although these small hydrocarbons are not obtained during the grafting reaction. This difference is probably related to the amounts of cyclopentadiene present and the different surface states of zeolite HY before and after modification. These results strongly support the above deduction.

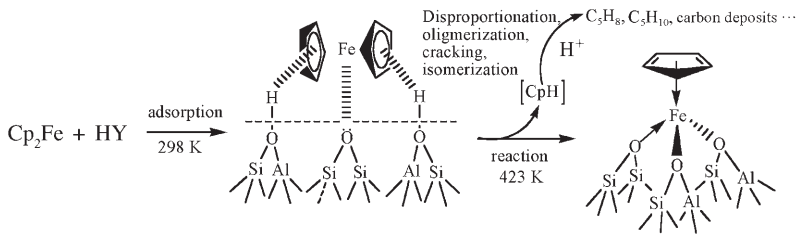

Scheme 1. Proposed pathway for the grafting reaction between ferrocene and HY zeolite.

The grafted complex is represented as $[(CpH)Fe(OZ\equiv)_3]$, where OZ is an ≡Si-O-Al(OSi)≡ unit in the zeolite framework. This is a 16-electron complex as the OZ group can be considered as a two-electron donor formally analogous, for example, to $CpHFe(CO)_3$, $(C_4H_4)Fe(CO)_3$, and

$(C_{10}H_{14}Fe(CO)_3)_2$.[48] A schematic representation of the grafted cyclopentadiene–iron complex is shown in Figure 9.

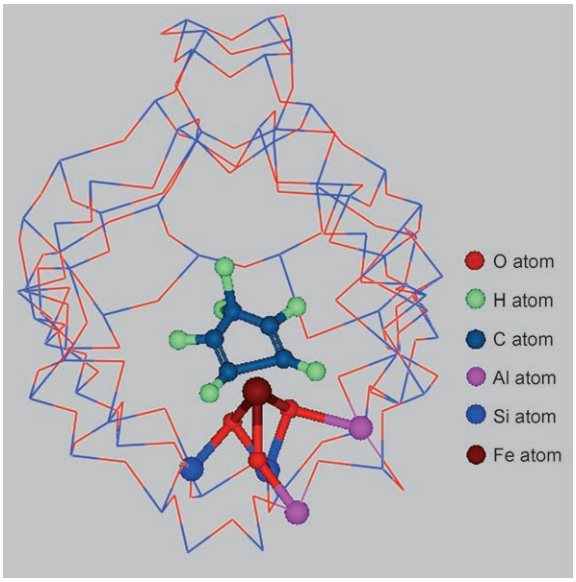

Figure 9. A schematic representation of the grafted iron cyclopentadiene complex.

Reactivity and uniformity of the surface [(≡Si-O-Al(OSi)≡)$_3$-Fe−(η^4-C_5H_6)] complex: HY zeolite dehydrated at 673 K contains three kinds of isolated OH groups, as shown by the OH stretching region of the IR spectrum. Consequently, the grafting reaction of ferrocene with acidic OH groups in the supercages of HY zeolite is close to an intermolecular reaction, as shown by the EXAFS results presented above, which demonstrate that the surface iron complex formed on Y zeolite remains mononuclear and does not undergo aggregation.

According to the 18-electron rule, this cyclopentadiene–iron surface complex should be unstable due to its unsaturated coordination, which means that it can coordinate with strong donors such as CO. Interestingly, upon addition of CO at room temperature, an unexpected IR band at 1707 cm^{-1} corresponding to a C=O bond is clearly observed. This observation, in combination with the disappearance of the band at 1491 cm^{-1} due to the CH_2 group and the absence of carbonyl bands in the region 1800–2100 cm^{-1}, indicates that CO does not bond to the iron atom of the surface iron species but probably inserts into the C−H bond of the CH_2 group to form a formylcyclopentadiene (C_5H_5CHO). To clarify the actual molecular structure formed, a TPD-MS investigation of this species was carried out. No C_5H_5CHO fragment is detected due to the facile thermal decomposition of C_5H_5CHO to form cyclopentadienyl radical and CHO[49] (see Figure S7 in the Supporting Information); other fragments of C_5H_5CHO, such as $C_5H_5^{\cdot}$, $CO^{\cdot}$, C_6H_4O, and $C_6H_3O^{\cdot}$, can, however, be detected. Additionally, the C=O absorption band of some ferrocene derivatives with CpCHO, such as formylcyclopentadienyl(cyclopentadienyl)iron (CpFe(CpCHO)) and formylferrocene, is also similar to that in our sample,[50] which suggests that the reaction of cyclopentadiene-iron with CO may result in the formation of C_5H_5CHO. The direct synthesis of C_5H_5CHO by the reaction of cyclopentadiene with CO has not yet been reported, although in a special environment, such as the surface of a zeolite, it is possible that a C_5H_5CHO species, like the cyclopentadiene-iron species, can form and coordinate to the iron atom. The role of iron seems be significant for this reaction. As shown in the IR spectra above (Figure 1), the strong interaction between iron and the active CH_2 group of cyclopentadiene weakens the C−H bond of the CH_2 group, which leads to splitting of the $\delta(CH_2)$ band, and means that CO can easily insert into the C−H bond to form an aldehyde. This results in the disappearance of the band at 1491 cm^{-1} corresponding to one of the vibrational modes of the CH_2 group. This insertion reaction is similar to the thermally mediated insertion of CO into vinylcyclopropanes in the presence of $Fe(CO)_5$.[51] The single carbonyl band is evidence for the near uniformity of the grafted iron species on the surface of the zeolite.

The surface iron complex is quite stable in vacuo or under an inert or hydrogen atmosphere below 473 K, and even under oxygen at room temperature. However, this organic ligand is easily oxidized at 323 K under oxygen, as shown by the remarkable change in the IR spectra (see Figures S4 and S5 in the Supporting Information). This thermal and chemical stability under these special conditions provides the surface iron complex a possibility of application. It is possible that the cyclopentadiene–iron complex could serve as a catalyst for the addition and insertion of cyclopentadiene or other dienes, a precursor of single-site iron oxide catalyst, or as a catalytic intermediate in catalytic [4+1] cycloaddition and iron-catalyzed Diels–Alder reactions.[52] Thus, a preliminary catalytic experiment has shown that iron-grafted Y zeolite prepared by removal of the surface cyclopentadiene ligand under O_2 is a good catalyst for the oxidation of alkenes. For example, it can rapidly oxidize propylene to CO_2 and CO at a low temperature of 393 K, as shown in Figure S7 in the Supporting Information). A study of the catalytic behavior of the cyclopentadiene–iron complex is currently in progress.

Conclusions

The acidic hydroxy groups in the supercages of HY zeolite can react with ferrocene at 423 K to form a surface [(≡Si-O-Al(OSi)≡)$_3$Fe(C_5H_6)] complex that is quite stable in vacuo or under an inert or hydrogen atmosphere below 473 K, and even under oxygen at room temperature. The XPS results indicate that iron is present in the divalent state after the grafting reaction, and the EXAFS data demonstrate that the grafted iron complex is mononuclear with each iron atom bonded, on average, to three oxygen atoms from the HY zeolite framework, with an Fe−O distance of 2.00 Å, and to five carbon atoms, with an Fe−C distance of 2.09 Å. The IR

spectra show that the species on the surface of HY zeolite is a cyclopentadiene–iron rather than a cyclopentadienyliron complex and that the cyclopentadiene ligand is easily oxidized under oxygen at a temperature of only 323 K. Reaction of the cyclopentadiene ligand with CO at room temperature provides possible evidence for the "molecular nature" of the iron-catalyzed [4+1] addition and insertion reactions.

Experimental Section

NH4Y zeolite, with a BET surface area of about 700 m^2g^{-1}, was purchased from Alfa Aesar. Its SiO_2/Al_2O_3 ratio is equal to 5.1. Ferrocene ($C_{10}H_{10}Fe$, 98%) was purchased from ACROS and purified by sublimation under vacuum prior to use. The Fe/Y sample used as XANES reference was obtained by calcination of the grafted sample at 773 K for 4 h.

Grafting reaction: The reaction of HY zeolite with ferrocene was performed in glassware connected to a vacuum line. The NH_4Y zeolite was first treated under flowing oxygen at 793 K for 20 h and then under vacuum (3×10^{-4} Torr) at 673 K for 3 h. This treatment removed all nitrogen from the solid (as indicated by IR spectroscopy) without destroying the structure (as checked by XRD) and the zeolite could be considered as a pure HY sample. DY zeolite was prepared by the exchange of HY zeolite dehydrated under vacuum at 373 K with D_2O.

After the mixture was cooled to room temperature, ferrocene was introduced onto the zeolite by sublimation. The system was then kept at 423 K for about 50 h to ensure complete reaction. The resultant solid was heated at the same temperature for 5 h under dynamic vacuum to eliminate physisorbed species, and was then sealed in a under vacuum in a glass tube. The grafting reaction of DY with ferrocene followed the same procedure.

Interactions of the surface species with CO and O_2: Reaction of the grafted sample with CO was performed in a closed home-made reaction cell with CaF_2 windows. After the grafting reaction and removal of the physisorbed species, highly pure CO or O_2 (99.999%) was injected into the reactor with a syringe. The reaction of the grafted sample with CO was monitored by IR spectroscopy.

Oxidation of propylene over iron-grafted Y zeolite: IR studies on the oxidation of propylene over Fe/Y zeolite were performed with a Nicolet 670 FT-IR spectrometer. The experiments were carried out in situ in a reaction cell equipped with two CaF_2 windows that are transparent in the IR region studied. Catalyst loading was 0.1 g. Propylene and oxygen were injected into the reactor in a 1:4.5 molar ratio with a syringe. The progress of the reaction was monitored by IR spectroscopy.

Structural characterization: X-ray photoelectron spectra (XPS) were measured with a Quantum 2000 spectrometer with monochromated $Al_{K\alpha}$ irradiation ($h\nu=1486.6$ eV). A sheet sample sealed in a glass tube was transferred and mounted on sample stubs with conductive carbon tape in a glove box. It was then cleaned by argon ion bombardment (1 kV) and spectra were recorded after 10-Å etching.

Temperature-programmed decomposition (TPD) and reduction (TPR) experiments were performed with an Autochem 2910 automatic catalyst characterization system equipped with an Omnistar GSD 30103 mass spectrometer. The sample loading was 0.2 g. The flow rate of the supporting gas (highly pure He (5N) for the TPD experiment and H_2/He (10%) for the TPR experiment) was 30 $mL\,min^{-1}$ and the heating rate was 5 $K\,min^{-1}$.

X-ray absorption spectra (Fe K-edge at 7.112 keV) were measured at the U7c station beam line of the Hefei Synchrotron Radiation Laboratory (NSRL, China) with stored electron energy of 0.8 GeV and ring currents of between 80 and 250 mA. The radiation was monochromated by using an Si(111) double-crystal monochromator in all cases. Data for the grafted sample and ferrocene absorbed on HY zeolite were collected in fluorescence mode at room temperature, while the data for ferrocene were recorded in transmission mode at room temperature with a sampling step of about 1.5 eV for XANES and 3.0 eV for EXAFS. The intensities of the incident and transmitted beams were monitored using two pure N_2- and 50% argon-doped N_2-filled ionization chambers, respectively. The energies of the samples were calibrated against an internal Fe foil standard by assigning the first inflection point to 7111.2 eV. The energy resolution was 0.3 eV.

Data treatment was carried out using the WinXAS 2.0 software package. A linear polynomial was fitted to the pre-edge region and a third-order polynomial to the post-edge region for background subtraction and XANES normalization, respectively. The radical structural function (RSF) FT [$k^3x(k)$] was obtained by Fourier transformation of the K^3-weighted experimental function $x(k)=(\mu(k)-\mu_0(k))/\mu_0(k)$ multiplied by a Gauss window in the range 2.6–13.4 $Å^{-1}$. The Fourier-filtered data were fitted in R-space in the range 1–2 Å. Phase shifts and backscattering amplitudes extracted from the reference material α-Fe_2O_3 (Fe–O) and ferrocene (Fe–C) were used to fit the EXAFS data to obtain the structural parameters of the complexes, including interatomic distances (R), coordination numbers (CN), Debye–Waller factors ($\Delta\sigma^2$), and edge energy shifts (ΔE_0). The validity of each fit was checked by fitting the K^3-weighted spectra in k-space, and the quality of each fit was estimated from the values of the variances of the imaginary and absolute parts of the FT.

Acknowledgments

This work was financially supported by the National Natural Science Foundation of China (grant nos. 20373011, 20673020, 20573020, and 20537010) and the National Key Basic Research Special Foundation, China (2004CCA07100). The authors thank Prof. Shiqiang Wei and Dr. Bo He from the Hefei Synchrotron Radiation Laboratory (NSRL; University of Science and Technology of China, Hefei) for collection, discussion, and analysis of the XAFS data.

[1] a) T. J. Donohoe, R. R. Harji, P. R. Moore, M. J. Waring, *J. Chem. Soc. Perkin Trans. 1* **1998**, 819–834; b) O. G. Kulinkovich, A. de Meijere, *Chem. Rev.* **2000**, *100*, 2789–2834; c) A. C. Comely, S. E. Gibson, S. Sur, *J. Chem. Soc. Perkin Trans. 1* **2000**, 109–124; d) *Transition Metal Reagents and Catalysis: Innovation in Organic Synthesis* (Ed.: J. Tsuji), Wiley-VCH, Weinheim, Germany, **2000**.
[2] T. J. Marks, *Acc. Chem. Res.* **1992**, *25*, 57–65.
[3] C. Copéret, M. Chabanas, R. P. Saint-Arroman, J. M. Basset, *Angew. Chem.* **2003**, *115*, 164–191; *Angew. Chem. Int. Ed.* **2003**, *42*, 146–181.
[4] J. C. Fierro-Gonzalez, S. Kuba, Y. Hao, B. C. Gates, *J. Phys. Chem. B* **2006**, *110*, 13326–13351.
[5] H. Ahn, T. J. Marks, US Patent No. 6235918, **2001**.
[6] G. G. Hlatky, *Chem. Rev.* **2000**,*100*, 1347–1376.
[7] a) K. Tsutsumi, H. Takahashi, *J. Phys. Chem.* **1970**, *74*, 2710–2713; b) E. Preuss, G. Linden, M. Peuckert, *J. Phys. Chem.* **1985**, *89*, 2955–2961; c) M. Niwa, K. Suzuki, K. Isamoto, N. Katada, *J. Phys. Chem. B* **2006**, *110*, 264–269; d) C. S. Triantafillidis, A. G. Vlessidis, N. P. Evmiridis, *Ind. Eng. Chem. Res.* **2000**, *39*, 307–319.
[8] C. Bolm, J. Legros, J. L. Paih, L. Zani, *Chem. Rev.* **2004**, *104*, 6217–6254.
[9] a) D. H. R. Barton, D. Doller, *Acc. Chem. Res.* **1992**, *25*, 504–512; b) D. H. R. Barton, *Chem. Soc. Rev.* **1996**, *25*, 237–239; c) D. H. R. Barton, *Tetrahedron* **1998**, *54*, 5805–5817; d) M. Fontecave, S. Ménage, C. Duboc-Toia, *Coord. Chem. Rev.* **1998**, *178–180*, 1555–1572; e) M. Costas, K. Chen, L. Que Jr. , *Coord. Chem. Rev.* **2000**, *200–202*, 517–544; f) M. Costas, M. P. Mehn, M. P. Jensen, L. Que Jr. , *Chem. Rev.* **2004**, *104*, 939–986; g) E. Y. Tshuva, S. J. Lippard, *Chem. Rev.* **2004**, *104*, 987–1012; h) D. Quinonero, K. Morokuma, D. G. Musaev, R. Mas-Balleste, L. Que Jr. , *J. Am. Chem. Soc.* **2005**, *127*, 6548–6549.
[10] a) W. Nam, M. H. Lim, H. J. Lee, C. Kim, *J. Am. Chem. Soc.* **2000**, *122*, 6641–6647; b) W. Nam, S. W. Jin, M. H. Lim, J. Y. Ryu, C. Kim,

Inorg. Chem. **2002**, *41*, 3647–3652; c) W. Nam, S. Y. Oh, Y. J. Sun, J. Kim, W. K. Kim, S. K. Woo, W. Shin, *J. Org. Chem.* **2003**, *68*, 7903–7906; d) C. M. Elliott, J. R. Dunkle, S. C. Paulson, *Langmuir* **2005**, *21*, 8605–8608; e) Z. Gross, S. Ini, *J. Org. Chem.* **1997**, *62*, 5514–5521.

[11] a) R. Bakhtiar, J. J. Drader, D. B. Jacobson, *J. Am. Chem. Soc.* **1992**, *114*, 8304–8306; b) R. C. Kerber, R. Garcia, A. L. Nobre, *Organometallics* **1996**,*15*, 5756–5758; c) S. Jiang, E. Turos, *Organometallics* **1993**,*12*, 4280–4282; d) F. Viton, G. Bernardinelli, E. P. Kundig, *J. Am. Chem. Soc.* **2002**, *124*, 4968–4969.

[12] a) B. M. Trost, *Science* **1991**, *254*, 1471–1477; b) B. M. Trost, *Angew. Chem.* **1995**,*107*, 285–307; *Angew. Chem. Int. Ed. Engl.* **1995**, *34*, 259–281.

[13] a) M. Iwamoto, H. Kusano, S. Kagawa, *Inorg. Chem.* **1983**, *22*, 3365–3366; b) M. Iwamoto, S. Nakamura, H. Kusano, S. Kagawa, *J. Phys. Chem.* **1986**, *90*, 5244–5249; c) A. L. Lapidus, M. M. Savel′ev, L. M. Muranova, S. D. Sominskii, L. T. Kondrat′ev, I. G. Borisovich, V. É. Vasserberg, *Russ. Chem. Bull.* **1985**, *94*, 18–22; d) C. Bowers, P. K. Dutta, *J. Phys. Chem.* **1989**, *93*, 2596–2603; e) J. Zwart, J. Vink, *Appl. Catal.* **1987**, *33*, 383–393.

[14] a) R. Shintani, K. Okamoto, Y. Otomaru, K. Ueyama, T. Hayashi, *J. Am. Chem. Soc.* **2005**, *127*, 54–55; b) J. F. Paquin, C. R. J. Stephenson, C. Defieber, E. M. Carreira, *Org. Lett.* **2005**, *7*, 3821–3824; c) M. D. Spencer, S. R. Wilson, G. S. Girolami, *Organometallics* **1997**, *16*, 3055–3067.

[15] P. A. Wender, M. P. Croatt, N. M. Deschamps, *Angew. Chem.* **2006**, *118*, 2519–2522; *Angew. Chem. Int. Ed.* **2006**, *45*, 2459–2462.

[16] M. S. Sigman, B. E. Eaton, *J. Am. Chem. Soc.* **1996**, *118*, 11783–11788.

[17] a) G. A. Ozin, D. M. Haddleton, C. J. Gil, *J. Phys. Chem.* **1989**, *93*, 6710–6719; b) G. A. Ozin, J. Godber, *J. Phys. Chem.* **1989**, *93*, 878–893.

[18] S. C. Mckinley, P. A. Vecchi, A. Ellern, R. J. Angelici, *Dalton Trans.* **2004**, 788–793.

[19] a) A. Borvornwattananont, K. Moller, T. Bein, *J. Phys. Chem.* **1989**, *93*, 4205–4213; b) K. Moller, A. Borvornwattananont, T. Bein, *J. Phys. Chem.* **1989**, *93*, 4562–4571.

[20] F. R. Sarria, O. Marie, J. Saussey, M. Daturi, *J. Phys. Chem. B* **2005**, *109*, 1660–1662.

[21] a) J. Brunvoll, S. J. Cyvin, *J. Organomet. Chem.* **1971**, *27*, 107–111; b) J. S. Bodenheimer, W. Low, *Spectrochim. Acta Part A*, **1973**, *29*, 1733–1743.

[22] a) D. M. Duggan, D. N. Hendrickson, *Inorg. Chem.* **1975**, *14*, 955–970; b) E. Maslowsky, *Vibrational Spectra of Organometallic Compounds*, Wiley, New York, **1977**.

[23] A. Svatos, A. B. Attygalle, *Anal. Chem.* **1997**, *69*, 1827–1836.

[24] X. Zhang, Y. Wang, F. Xin, *Appl. Catal. A: Gen.* **2006**, *307*, 222–230.

[25] F. Heinrich, C. Schmidt, E. Löffler, M. Menzel, W. Grünert, *J. Catal.* **2002**, *212*, 157–172.

[26] M. F. Ruiz-Lopez, M. Loos, J. Goulon, M. Benfatto, C. R. Natoli, *Chem. Phys.* **1988**, *121*, 419–437.

[27] N. Rösch, K. H. Johnson, *Chem. Phys. Lett.* **1974**, *24*, 179–184.

[28] S. H. Choi, B. R. Wood, J. A. Ryder, A. T. Bell, *J. Phys. Chem. B* **2003**, *107*, 11843–11851.

[29] X. Wang, J. Long, G. Yan, X. Fu, P. Liu, J. M. Basset, F. Lefebvre, *Microporous Mesoporous Mater.* in press, DOI:10.1016/j.micromeso.2007.03.047.

[30] B. J. Iball, C. H. Morgan, *Acta Crystallogr.* **1967**, *23*, 239–244.

[31] M. R. Churchill, J. Wormald, D. A. T. Young, H. D. Kaesz, *J. Am. Chem. Soc.* **1969**, *91*, 7201–7203.

[32] a) P. E. Riley, R. E. Davis, *Inorg. Chem.* **1975**, *14*, 2507–2514; b) R. M. Moriarty, K. N. Chen, C. L. Yeh, J. L. Flippen, J. Karle, *J. Am. Chem. Soc.* **1972**, *94*, 8944–8946; c) F. A. Cotton, P. Lahuerta, *Inorg. Chem.* **1975**, *14*, 116–119.

[33] R. P. Dodge, V. Schomaker, *Acta Crystallogr.* **1965**, *21*, 614–617.

[34] J. A. Connor, L. M. R. Derrick, I. H. Hillier, *J. Chem. Soc. Faraday Trans 2* **1974**, *70*, 941–944.

[35] C. R. Brundle, T. J. Chuang, K. Wandelt, *Surf. Sci.* **1977**, *68*, 459–468.

[36] R. B Woodward, M. Rosenblum, M. C. Whiting, *J. Am. Chem. Soc.* **1952**, *74*, 3458.

[37] a) M. A. Shaul, H. L. Morton, *J. Organomet. Chem.* **1970**, *22*, 171–177; b) R. L. Schaaf, C. T. Lenk, *J. Org. Chem.* **1963**, *28*, 3238–3240; c) J. R. Pladziewicz, J. H. Espenson, *Inorg. Chem.* **1972**, *11*, 3136–3138; d) A. M. Bond, T. L. E. Henderson, D. R. Mann, T. F. Mann, W. Tormann, C. G. Zoski, *Anal. Chem.* **1988**, *60*, 1878–1882.

[38] P. K. Dutta, M. A. Tomson, *Chem. Phys. Lett.* **1986**, *131*, 435–437.

[39] T. Youko, I. Shinichi, I. Ryuichi, *J. Phys. Chem. Solids* **2004**, *65*, 471–473.

[40] a) R. K. Kochhar, R. Pettit, *J. Organomet. Chem.* **1966**, *6*, 272–278; b) R. Prins, A. R. Korswagen, A. G. T. G. Kortbeek, *J. Organomet. Chem.* **1972**, *39*, 335–344.

[41] P. Dufour, S. L. Scott, C. C. Santini, F. Lefebvre, J. M. Basset, *Inorg. Chem.* **1994**, *33*, 2509–2517.

[42] P. J. Wilson, Jr., J. H. Wells, *Chem. Rev.* **1943**, *43*, 1–50.

[43] G. Spoto, A. Zecchina, S. Bordiga, R. Dante, *Mater. Chem. Phys.* **1991**, *29*, 261–269.

[44] T. Maschmeyer, F. Rey, G. Sankar, J. M. Thomas, *Nature* **1995**, *378*, 159–162.

[45] P. E. Sinclair, G. Sankar, C. R. A. Catlow, J. M. Thomas, T. Maschmeyer, *J. Phys. Chem. B* **1997**, *101*, 4232–4237.

[46] a) J. R. Anderson, Y. F. Chang, R. J. Western, *J. Catal.* **1989**, *118*, 466–482; b) N. R. Avery, *J. Electron Spectrosc. Relat. Phenom.* **1986**, *39*, 1–9.

[47] a) S. Gopal, P. G. Smirniotis, *J. Catal.* **2002**, *205*, 231–243; b) Y. K. Chua, P. C. Stair, *J. Catal.* **2003**, *213*, 39–46.

[48] a) G. F. Emerson, L. Watts, R. Pettit, *J. Am. Chem. Soc.* **1965**, *87*, 131–133; b) J. D. Fitzpatrick, L. Watts, G. F. Emerson, *J. Am. Chem. Soc.* **1965**, *87*, 3254–3255; c) H. Yasuda, Y. Ohnuma, M. Yamauchi, *Bull. Chem. Soc. Jpn.* **1979**, *52*, 2036–2042.

[49] D. Hodgson, H. Y. Zhang, M. R. Nimlos, J. T. Mckinnon, *J. Phys. Chem. A* **2001**, *105*, 4316–4327.

[50] a) P. J. Graham, R. V. Lindsey, G. W. Parshall, M. L. Peterson, G. M. Whitman, *J. Am. Chem. Soc.* **1957**, *79*, 3416–3420; b) S. I. Goldberg, *J. Org. Chem.* **1960**, *25*, 482–483.

[51] M. M. Schulze, U. Gockel, *J. Organomet. Chem.* **1996**, *525*, 155–158.

[52] a) P. V. Bonnesen, C. L. Puckett, R. V. Honeychuck, W. H. Hersh, *J. Am. Chem. Soc.* **1989**, *111*, 6070–6081; b) T. R. Kelly, S. K. Maity, P. Meghani, N. S. Chandrakumar, *Tetrahedron Lett.* **1989**, *30*, 1357–1360; c) A. S. Olson, W. J. Seitz, M. M. Hossain, *Tetrahedron Lett.* **1991**, *32*, 5299–5302.

Received: April 2, 2007
Published online: July 4, 2007

